Lab on a Chip

Rapid Cell Isolation in Breastmilk in a Non-Clinical Setting by a Deterministic Lateral Displacement Device and Selective Water and Fat Absorption

Journal:	*Lab on a Chip*
Manuscript ID	LC-ART-10-2023-000899.R1
Article Type:	Paper
Date Submitted by the Author:	12-Dec-2023
Complete List of Authors:	Hawkins, Jamar; University of Massachusetts Amherst, Mechanical and Industrial Engineering Browne, Eva; University of Massachusetts Amherst, Department of Veterinary and Animal Science Arcaro, Kathleen; University of Massachusetts Amherst, Department of Veterinary and Animal Science Sun, Yubing; University of Massachusetts Amherst, Mechanical and Industrial Engineering

Rapid Cell Isolation in Breastmilk in a Non-Clinical Setting by a Deterministic Lateral Displacement Device and Selective Water and Fat Absorption

Jamar Hawkins[1], [2]Eva P. Browne, [2]Kathleen F. Arcaro, and Yubing Sun[1,3]

[1]Department of Mechanical and Industrial Engineering, University of Massachusetts, Amherst, Massachusetts 01003, USA.
[2]Department of Veterinary and Animal Sciences, University of Massachusetts, Amherst, Massachusetts 01003, USA.
[3]Department of Biomedical Engineering, University of Massachusetts, Amherst, Massachusetts 01003, USA.

*Correspondence should be addressed to and Y. Sun (ybsun@umass.edu)

ABSTRACT

Breastmilk is a reliable source of biomarker-containing, sloughed breast cells that have the potential to give valuable health insights to new mothers. Furthermore, known DNA-based markers for pregnancy-associated breast cancer are chemically stable and can be safely stored on a commercially available FTA® Elute Micro (EM) card, which can subsequently be mailed to a testing facility for the cost of a stamp. In theory, this archiving process can be performed by nonprofessionals in very low-resource settings as it simply requires placing a drop of breastmilk on an EM card. Although this level of convenience is paramount for new mothers, the low cell density of breastmilk complicates archiving on an EM card as such commercial products and associated protocols were designed for high-cell density physiological fluids such as blood. In this study, we present the use of a Deterministic Lateral Displacement (DLD) device combined with porous superabsorbent polymers and hydrophobic sponges to achieve simple and low-cost cell enrichment in breastmilk. As the critical separation diameter in a DLD device is more heavily dependent on lithographically controlled pillar layout than fluid or flow properties, our use of DLD microfluidics allowed for the accommodation of both varying viscosities in human breastmilk samples and a varying pressure of actuation resulting from manual, syringe-driven operation. We demonstrate successful cell enrichment (>11×) and a corresponding increase in the DNA concentration of EM Card elutions among breastmilk samples processed with our hybrid microfluidic system. As our device achieves sufficiently high cell enrichment in breastmilk samples while only requiring the user to push a syringe for 4 min with reasonable effort, we believe that it has high potential to expand EM card DNA archiving for diagnostic applications with low-cell density physiological fluids and in low-resource settings.

INTRODUCTION

Within 5 years of childbirth, a woman's risk of breast cancer is reported to be almost double that of a nulliparous woman of the same age[1]. Furthermore, several reports demonstrate that women diagnosed with breast cancer within that timeframe have significantly higher rates of distant recurrence (metastasis)[2, 3] and mortality[4]. For this reason, breast cancer detected within five years of childbirth, otherwise known as pregnancy-associated breast cancer, is recognized as a distinct and especially lethal type of breast cancer. Fortunately, several recent reports indicate that early detection of breast cancer markers within native breast cells is a promising strategy for early detection and improving survival rates[5-7].

Human milk contains multiple cell types, including epithelial, immune, and stem cells[8-10]. The majority of human cells in milk are epithelial cells. Gleeson *et al.* used a combination of flow cytometry and single cell RNA-sequencing to characterize 6 populations of epithelial cells in milk (~93%) and smaller populations of immune cells and stem cells (~7%)[9]. Testing for breast cancer markers in cells found in breastmilk is an exciting possibility as nursing women can express breastmilk naturally without any need for expert assistance. As such tests mainly involve the analysis of methylation patterns or mutations of chemically stable genomic DNA of epithelial cells in breastmilk[11], time between sample collection and analysis is noncritical if samples are properly stored. Theoretically, these loose requirements allow convenient and continuous screening over time as these DNA samples can be archived from home and mailed to a lab for testing. As newborn children require a great deal of care, this option could be very convenient for new mothers and increase the accessibility of breast cancer screening altogether. However, making this process sustainable and inexpensive presents the engineering challenge of getting a sufficient number of cells from breastmilk, which has a very low cell density, without excess liquid that can foster bacterial growth and compromise downstream testing. Although

expedited shipping of large quantities of milk in refrigerated containers is a viable option to circumvent bacterial growth, this process is costly and would greatly restrict access to the intervention.

For long-term dry storage and transport of DNA at room temperature, cells can be lysed directly on commercially available DNA collection cards such as FTA® Elute Micro (EM) cards on contact, which allow for the selective, water-based elution of nucleic acids by using chaotropic salts to keep proteins tightly bound. However, there remains the challenge of getting a sufficient DNA template (~ 1 μg) from breastmilk samples as only microliter volumes can be added to the cards. This is due to the low cell number and large variation in breastmilk. Using a combination of flow cytometry and microscopy, a recent study found that 1 mL of milk comprises 1.2×10^4 human cells with a range of 0.06×10^4 to 1.2×10^5, depending on the milk donor and other factors[8]. As EM cards hold 12 - 40 μL of sample per spot, which would be equivalent to 1,440 to 4,800 human milk cells or less than 30 ng DNA per spot, unprocessed samples do not provide sufficient DNA for the downstream DNA methylation analyses. To accurately assess breast health, DNA from cells representing the entire mammary gland must be obtained. Our previous works have shown that the human cells in 1 - 2 mL of milk are sufficient for global DNA methylation analyses[6, 12]. To achieve this goal, a prior cell-spiking intervention is needed to address the issue of low cell density. Large and expensive centrifuges typically used for cell separation are costly to purchase and transport. To enable point-of-care applications, several research groups have designed microfluidic devices to achieve cell separation and enrichment. For example, Li et al. designed acoustofluidic devices[13], which generate pressure nodes to organize and separate cells by size. Di Carlo *et al.* designed tortuous microfluidic channels[14], which use inertial focusing to flow cells in streamlines. Unfortunately, the

requirement of pumps, flow regulators, noisy transducers, and waveform generators makes these devices difficult to incorporate in an at-home/low-resource setting. An additional challenge with this application is the variation in fluid properties. Unlike commercial cell culture media, breastmilk samples can vary significantly in viscosity, cell density, and fat content. Therefore, specific flow parameters cannot be assumed to the required accuracy of the aforementioned devices.

Deterministic lateral displacement (DLD) devices present a promising solution to this challenge as they have been demonstrated as effective cell separators under various flow rates with minimal equipment required[15, 16]. In early studies on DLD devices, Davis proposed an equation for critical separation diameter based on a best fit model of empirical data found from testing with circular pillars: $D_c = 1.4G\varepsilon^{0.48}$,where D_c is critical separation diameter, G is the vertical gap between two pillars, and ε is the row shift fraction[17]. More recently, Zhang *et al*. used fluid simulation to determine a general equation for critical separation diameter accounting for pillar shape: $D_c = \alpha G\varepsilon^{\beta}$, where α and β are two geometric parameters that change with the shape and arrangement of the pillars[18]. Interestingly, these equations imply a high degree of leniency for other parameters such as viscosity and flow rate within a laminar flow regime. A very telling example is a triangular DLD device designed by Lutherback *et al*. which demonstrates effective cell separation at various flow rates with the highest being 10 mL/min[19], suggesting that DLD devices have potential for rapid cell separation at relatively high flow rates.

While DLD devices have been widely used for cell separation in water-based solutions (*e.g.*, PBS, culture media, etc.), they have not been applied to breastmilk. In this study, we aim to design a robust and inexpensive system to enrich cells in breastmilk, which will then be lysed on EM cards directly for DNA collection and storage. We found that using merely a DLD device

could not enrich cells to desirable concentrations. Here, we combined a DLD device with porous superabsorbent polymers (PSAPs), a low-cost material for water absorption, and PDMS sponges for fat removal, and successfully developed a simple workflow (**Figure 1**) to collect sufficient DNA samples on DNA collection cards for breast cancer risk screening. Our approach requires minimal equipment and user expertise, and resolves logistical issues (bacterial contamination, shipping costs, etc.) in the procurement of participant samples for DNA analysis.

METHODS

Milk Viscosity Measurements

Viscosity measurements were made using a 0.55 mm inner diameter Ostwalt viscometer. Viscosity values were calculated using ultrapure Milli-Q water as a reference. In this and following experiments, milk samples from three different donors were tested.

DLD Device Design

Our DLD array was designed to accommodate cells 9-20 μm in diameter according to the aforementioned equation initially proposed by Zhang et al[18]. We used a vertical gap size of 42 μm, lateral shift of 1/20, pillar base of 48.33 μm, and pillar height of 70 μm for a critical separation diameter of ~9 μm.

Device Fabrication

Microfluidic devices were designed in KLayout and printed on a 5” soda-lime glass photomask with a Heidelberg DWL200 laser writer. In a contact mask aligner, the pattern was transferred to the positive photoresist AZ10XT (Microchemicals, Ulm Germany), which was spun onto a 4” silicon wafer. Deep Reactive Ion Etching (DRIE) was performed on the uncoated portions of the

wafer with an SPTS Rapier to a total depth of 70 μm. The etched wafer was silanized overnight using 50 μL of perfluorooctyltrichlorosilane (Alfa Aesar, Haverhill MA). PDMS prepolymer containing elastomer base and curing agent (10:1 w/w; Sylgard 184, Dow-Corning) was thoroughly mixed for 5 mins and degassed for 30 mins before the PDMS was poured onto the etched silicon wafer. The PDMS was placed in an oven at 110ºC for 20 mins, peeled from the silicon wafer, had holes punched through the inlet and outlet ports, sonicated in 100% ethanol for 30 mins, and was thoroughly dried with Dust-Off® compressed air (Falcon Safety Products NJ USA) before it was finally bonded to a glass slide using a house-made oxygen plasma cleaner.

100% Ethanol was pulled through the device with a syringe for 1 min to effectively wet the inner channels of the device and clear any residual debris or obstruction. The device was then submerged in a petri dish of PBS and had 2% Pluronic F127 in PBS flowed through for 1 min to clear out ethanol. The Pluronic F127 was left in the device while incubated at 37ºC in a humidified environment for 20 mins to ensure poloxamer coating to the hydrophobic PDMS substrate. Finally, devices were flushed thrice with DI water to remove unbound poloxamer and stored at 4ºC until experiments began.

Absorbent Microfilter Beads

Polymer microfilter beads were created using a similar protocol to that initially described by Chen *et al*.[20]. A solution of 15% Polyethylene Glycol (w/w), 0.2% Methylene Bisacrylamide (w/w), 6% Sodium Acrylate (w/w) and 4% Acrylamide (w/w) in DI water was dissolved via ultrasonication for 20 minutes. The mixture was then degassed for 10 mins prior to being added to a 0.3% Ammonium Persulfate solution in DI water and thoroughly mixed. 300 μL of the resulting mixture was added to each well of a 96-well plate. The well plate was sealed with an aluminum film and placed inside a water bath at 75ºC for 30 mins to allow curing. Upon removal

from the water bath, the beads were taken from each well with tweezers and submerged into 100% ethanol for 30 mins to dissolve the porogen (PEG). Lastly, the beads were then placed into an oven at 60ºC overnight to allow dehydration.

Cell and Waste Outlet Flow Analysis

1 mL of PBS spiked with Madin-Darby canine kidney (MDCK) cells to a concentration of 100,000 cells/mL was flowed through the DLD device at a rate of 100 μL/min and collected in two separate Eppendorf tubes connected to either the cell or waste outlet. The mass of PBS in each tube is measured on a scale and then recorded. The cell concentration of each outlet was measured with a hemacytometer. During experiments involving a centrifuge group, the solution was centrifuged at 1200 rpm for 5 mins and the cell pellet was resuspended in 125 μL of PBS or breastmilk.

Flow Rate Parameterization Experiments

1 mL of PBS was spiked with MDCK cells to a concentration of 100,000 cells/mL and flowed through the DLD device at a flow rate of either 10 μL/min, 100 μL/min, 1 mL/min or 5 mL/min using a Harvard Apparatus Pump 33 DDS (Harvard Apparatus, Holliston, MA). PBS collected from the cell outlet of the device had its cell concentration measured with a hemacytometer.

DNA Elution from EM Cards and Spectrophotometer Measurements

Two 3mm biopsy punches were taken from each sample area on an EM card and placed into individual 1.5 mL Eppendorf tubes, which were then placed into a heat block at 80ºC for 20 mins. After heating, the Eppendorf tubes had 500 μL of sterile water added and were then vortex mixed for 5 seconds. The two punches were promptly transferred to a new 1.5 mL Eppendorf tubes containing 100 μL of sterile water. The tubes were placed into a thermomixer set to 95ºC

and 500 rpm for 30 mins to allow for DNA elution from the punches. Following this step, the Eppendorf tubes were vortexed for 60 seconds and had their two punches discarded prior to a 2 min centrifuge at 14100 rcf to pellet any residual paper fibers to the bottom of the tube. 80 µL of supernatant was transferred to a new Eppendorf tube and had 200 µL of ice cold 100% ethanol, 8 µL of 3M Sodium Acetate, and 0.75 µL of Glycol Blue added. The solution was vortexed for 10 seconds and left at -20ºC overnight to allow DNA precipitation from the solution. DNA was then pelleted via centrifugation at 15300xg for 30 mins at 4ºC. Supernatant was discarded and the pellet was resuspended in ice cold, 70% ethanol and vortexed for 10 seconds prior to another centrifugation at 15300×g for 30 mins at 4ºC. To further ensure removal of the chaotropic salts from the EM Cards, the pellet was again washed with 70%, ice cold ethanol and centrifuged at 15300×g for 30 mins at 4ºC prior to being resuspended in 70µL of sterile, ultrapure water. 2 µL of the elution was placed onto a pedestal on a Nanodrop 8000 (Thermofisher, Waltham, MA) and measured at 230 nm, 260 nm, and 280 nm to quantify the background, nucleic acid, and protein content, respectively.

Real Time-PCR

Quantitative (real time) PCR was run using the BioRad Thermocycler C1000 Touch-CFX96 Real-Time System with the TaqMan Universal Master Mix II (MM) (Applied Biosystems) and the following primers and probe for ALU. Forward primer: ATCACGAGGTCAGGAGATCGAG; Reverse primer: CCGGCTAATTTTTGTATTTTTAGTAGAGA;
Probe: 6FAM-ATCCCGGCT/ZEN/AACACGGTGAAACCC-IBFQ. All samples were run in technical duplicates. Briefly, 1 µL genomic DNA (concentration $\leq$ 50 ng/µL) was added to each

well which already had 29 μL MM and run with the following settings: 95°C for 10 min, followed by 36 cycles of 95°C for 15 sec, 60°C for 60 sec. A six-point standard with known concentrations and a negative control were run on each plate in duplicate. DNA concentrations of samples were calculated from the standard curve.

Statistical Analysis

Statistical analysis was performed using Origin Pro. For statistical comparations between two data sets, P-values were calculated using the student t test function. For statistical comparations between three or more data sets, P-values were calculated using the one-way ANOVA with Tukey post hoc analysis. In bar plots, data represent mean ± standard error of mean (s.e.m).

RESULTS

Fluid Modeling and Device Design

Our envisioned process of efficient DNA collection from breastmilk involves the use of an intermediate microfluidic cell enrichment step prior to transferring to an EM card **(Figure 1)**. Breastmilk can be considered an oil-in-water emulsion with fat globules serving as the dispersed phase[21]. As the exact ratio of the dispersed and continuous phase (water) of breastmilk can vary even within milk expressed from the same breast at different times, an exact viscosity of breastmilk for our application cannot be easily defined. Ostwalt viscometer measurements of three donor breastmilk samples gave a range of viscosity values between (1.40 – 1.77 cp) and an average viscosity of approximately 1.68 cp, significantly higher than that of water (1 cp). Although we employed a DLD design with the intention of minimizing the effect of fluid properties on the efficacy of our separation, the viscosity of the fluid impacts the pressure

requirements and Reynold's number of the flow. Therefore, we designed our DLD system using triangular pillars because prior works have shown that triangular pattern allows gaps between pillars to be 20-30% higher than that of the standard circular patterns at the same critical separation diameter[18, 19]. This design will allow us to achieve a higher throughput at similar pressure drops to accommodate the increased viscosity of breastmilk relative to the typical fluids like water and culture media used in prior DLD devices.

Our DLD device has a single inlet channel and two outlets (cell and waste). The cell outlet was in the center of the device, where the DLD device was designed to guide the flowing cells **(Figure 2A)**. The waste outlet was connected to 10 channels near the cell outlet which were intended to collect fluid with minimal cell concentration **(Figure 2A).** The dimensions and arrangement of the DLD pillars were tailored towards our specific fluid and cell types. Human milk is reported to contain a variety of cell types of various sizes, the largest of which are 9-18μm diameter leukocytes[22]. Our DLD device featured gaps of 42 μm in order to comfortably accommodate these cells, despite our sole target being much smaller sloughed epithelial cells, to ensure the device would not be obstructed during operation **(Figure 2A)**. To balance liquid throughput and pillar stiffness, we selected a pillar height of 70 μm.

DLD Device Fabrication and Assembly

The DLD triangular arrays were successfully fabricated in PDMS using soft lithography with etched wafers as templates **(Figure 2A)**. The devices were washed in ethanol, bonded to glass slides, and coated with Pluronic F127 as described in the methods section. Devices were able to be cleared of any residual debris from fabrication prior to experimentation by syringe-pulling ethanol through the DLD microchannel.

Mass Flow Rate Analysis

To collect sufficient cells for reliable PCR analysis within limited volume allowed on EM cards, we estimated that an eight-fold increase in the cell concentration was desirable. Though the triangular pillars featured in the device were designed to guide cells to the cell outlet, the cell concentration of solution from the cell outlet still heavily depended on the volume of liquid exiting the cell outlet. An understanding of the mass flow rate through both output ports was required to enable a thorough analysis of the cell separation efficacy and design a protocol that achieves the target cell concentration in a volume the EM cards can accommodate. To determine these critical parameters of our device, we flowed PBS, spiked with MDCK cells which have similar size to breast epithelial cells, to an initial concentration of 100,000 cells/mL, at a rate of 100 μL/min through our DLD device and into two separate Eppendorf tubes (cell or waste) for 10 mins **(Figure 2B,** see **Methods** for details**)**. We found that the average mass flow rate into the cell outlet was ~14.2% of the average flow rate out of the device **(Figure 2C**). In contrast, the cell concentration of the PBS collected from the cell outlet was ~50 times that of the waste outlet, suggesting cells were successfully focused to the central cell outlet **(Figure 2D, Supplementary Video 1)**.

Cell-Spiking Efficacy of the DLD Device

Although the mass flow rates leaving the cell and waste outlet of our DLD device provided valuable insights into the potential efficacy of cell enrichment, we further evaluated the efficacy of separation of our DLD device by direct comparison with a gold standard (centrifuged) and nonintervention group (*status quo*). For this experiment, we first prepared 1mL PBS solutions spiked with MDCK cells at the concentration of 100,000 cells/mL. In our DLD group, we flowed 1 mL cell-spiked PBS solution at 100 μL/min flow rate through the DLD device. We quantified

outcomes by counting the cell number in 125 µL of post-processed solution, typically used for 3 spots on EM cards (40 µL per spot). As discussed above, at least 100,000 cells in this 125 µL solution are required for proposed DNA methylation analysis. The cell concentrations in the cell outlet and the waste outlet were compared with a *status quo* group and a centrifuged group (1mL cell-spiked PBS centrifuged at 1200 rpm for 5 minutes, pellets resuspended in 125 µL PBS). Cells could be observed flowing to the cell outlet without any clogging between the gaps of the pillar array **(Figure 3A)**. We found the cell concentration from the cell outlet to be around 4.5× the *status quo*, further verifying that the pillars of the device are guiding the cells to the cell outlet **(Figure 3B)**. Expectedly, the centrifuge group outperformed the DLD device group by about 30%. Notably, cell concentration in the DLD and status quo group will not change with increasing total volume of samples but will scale proportionally in the centrifuged group.

Determining Effect of Flow Rate on DLD Cell Separation

The 100 µL/min flow rate used in the previous experiment was ideal for observing individual cells moving through our DLD device, but too slow for getting a sufficient sample volume to fill all four 40 µL spots of one EM card. To determine if our device is suitable for manual syringe-driven actuation, we next evaluated how effective our DLD device was at various flow rates so we could understand if higher flow rates could be used without compromising separation efficacy and how reasonable deviations in user operation (force of actuation) affects the separation efficiency of our DLD device.

Based on our empirical findings on the difficulty of pushing fluid through our DLD device, we identified a range of 10 µL/min – 5 mL/min to encapsulate the flow rates resulting from reasonable effort of syringe pushing. Using a syringe pump, PBS spiked with MDCK cells to a concentration of 100,000 cells/mL was flowed through the device at either 10 µL/min, 100

μL/min, 1 mL/min, and 5 mL/min (**Figure 3C**). We found that the cell concentration in the cell outlet remained around 60,000 cells/125 μL in all cases, suggesting the robustness of our device regarding a broad range of flow rates (**Figure 3D**).

Cell Concentration Spiking of DLD Device Augmented with Absorbent Polymer Post-Processing

As the DLD device has been demonstrated to achieve a 6:1 ratio of mass flow rate between the waste and cell outlets, the maximum theoretical value of cell-spiking is capped at 7×. As shown in **Figure 3B**, the actual cell spiking ratio was about 4.5×. To achieve our goal of an 8× increase in cell concentration without significantly sacrificing the throughput of the device, we employed dehydrated porous superabsorbent polymer (PSAP) beads as a low-volume post-processing method in our cell collection reservoir **(Figure 4A-D)**. PSAPs have demonstrated potentials as an enrichment method for cells, extracellular vesicles, and proteins[20, 23-25]. These polymer beads are "self-driven" and utilize sized-based exclusion to selectively intake water and very small particles. Not only does this offer the advantage of removing cell-free fluid, but also allows tuning to facilitate protein uptake thus increasing DNA purity downstream. This combination is intuitive and convenient as both interventions can operate simultaneously without interfering with one another. Prior to testing the PSAP beads for their cell-spiking efficacy, we investigated their liquid absorption over 20 minutes by placing them individually into wells of a 24-well plate filled with either breastmilk or PBS. We found that within 10 mins the beads were able to absorb about 150 μL of PBS and about 125 μL of breastmilk **(Figure 4E)**.

We next sought to investigate if the combination of PSAP beads and DLD device can achieve targeted cell concentration. For this experiment, we had 4 mL of cell-spiked PBS flowed through our device at an average flow rate of 1 mL/min into one well of a 24-well plate containing 3 PSAP beads (B-DLD group in **Figure 4F**). Upon completion, the measurement of

cell density was delayed for 10 minutes to allow passive PSAP bead spiking. Similarly, we included a s*tatus quo* control group (no intervention) and a centrifuged group (4 mL of cell-spiked PBS centrifuged and resuspended into 125 μL of PBS). Although still significantly outperformed by the centrifuge group, the B-DLD group showed about an 11× increase in cell concentration compared to that of the *status quo* group and surpassed our targeted 8× cell spiking ratio **(Figure 4F)**. Notably, increasing the total volume of sample processed can effectively increase the cell concentration for the centrifugation methods (as shown in **Figure 4F** and **3B**), however, without introducing absorption beads, the DLD device results in a relatively constant output cell concentration.

Determining Hybrid Device Efficacy in Breastmilk

As we successfully achieved our target cell spike in PBS, we could assert that the hybrid device works as intended for fluids with similar density and viscosity to water. This finding provided a point of reference for us to determine how the heterogeneity and viscosity of human breastmilk affects the efficacy of separation in our DLD device. We thus next tested the device efficacy by spiking MDCK cells or MCF-7 breast cancer cells in breastmilk samples. The complexity of milk drastically complicated imaging; however, we were able to observe spherical objects that were too large (~30 μm diameter) to be MDCK cells exiting the cell outlet (**Figure 5A, Supplementary Video 2**). Further observation at the cell outlet collection well led us to conclude that they were coalesced milk fat globules. To better visualize the cell trajectory, we used GFP-tagged MCF-7 cells (**Figure 5B, Supplemental Video 3**). From fluorescent imaging, cells seemed to be successfully reaching the cell outlet of the DLD device, however the milk fat globules entering the same channel warranted additional intervention. This is because the PSAP

beads cannot absorb oil and were therefore not suitable to completely achieve the same extent of post-processing of breastmilk as in PBS.

To resolve the issue of milk fat globules entering the cell outlet, we created PDMS sponges using store-bought sugar cubes as sacrificial templates **(Figure 5C,** see **Methods** for details**)**. The small pores in the hydrophobic PDMS serve as a filter and facilitate selective uptake of the oily milk fat globules **(Figure 5D)**. PDMS sponges were cut into 3mm diameter and 6 mm long cylinders and placed into the 24-well plate to which the cell collection outlet was flowed.

We next tested the performance of the DLD device alone, DLD device with beads, and DLD device with both beads and sponges in PBS or breastmilk spiked with MDCK cells at a concentration of 100,000 cells/mL (**Figure 5E**). In this experiment, we again used a flow rate of ~1 mL/min to process 4 mL of samples and 3 PSAP beads and 3 PDMS sponges were used to sufficiently remove water and oil contents, respectively in corresponding experimental groups. After 4 mL of breastmilk was flowed through the DLD device, the beads and sponges at the cell outlet were left to absorb for 15 mins before 40 μL of the spiked solution was added onto a sample area of an EM card. For comparison, 4 mL of breastmilk spiked to the initial concentration of 100,000 cells/mL was centrifuged, resuspended in 125 μL, and had 40 μL placed onto a sample area of an EM card (centrifuge) while an additional group was spiked to the same initial concentration simply had 40 μL removed and placed on a sample area of an EM card (*status quo*).

A main concern about the timeliness of cell-enrichment is the window for bacterial growth. Distinguishing between human and bacterial DNA was essential to verifying that any increase in DNA concentration was the result of our device enriching the cells of interest. To get an

understanding of any potential background signals from the human breastmilk, we employed real time-PCR amplification of the *ALU* gene, which exists only in primates, to quantify the DNA concentrations (**Figure 5F**). This allowed for both a clear understanding of the background signal resulting from human DNA present in the samples prior to the initial spiking and allowed us to exclude any DNA from bacteria present in the experimental groups. Interestingly, we see no significant difference in the DNA concentration among our milk blank (no added cells) and cell-spiked controls **(Figure 5F)**. However, we observe that the device group enriched using beads and sponges has about a 20 ng/μL concentration. As each punch is eluted in 50 μL of ultrapure water, this result indicates that the amount of DNA from solely the MCF-7 cells roughly hit our target mass of 1 μg.

In our experiments with MDCK cells, quantification of DNA concentration on EM cards indicated the hybrid DLD device group (DLD combined with PSAP beads and PDMS sponge) had about 13× the DNA of the *status quo* group (~20 ng/μL) **(Figure 5F)**. Interestingly, the fold changes between the centrifuge groups and hybrid DLD device groups in both fluids is much less than what was seen in our hemocytometer cell counts (**Figure 4F),** likely due to the centrifuge group exceeding some capacity limitation of the EM cards. As the lysing and DNA storage of the cards depends on their chemical treatment, it is plausible that the high number of cells used in the centrifuge group overwhelmed the cards.

DISCUSSION

While cell separation strategies have been extensively explored, cell enrichment followed by DNA extraction from breastmilk samples, particularly in resource-limited settings, have not been achieved. As breastmilk is heterogeneous, viscous, and fat-enriched, conventional cell separation

strategies designed for culture media or blood samples cannot be directly applied. In our work, we reported three strategies for cell enrichment from breastmilk samples, *i.e.*, DLD-based microfluidic device, water-absorbing PSAP beads, and fat-absorbing PDMS sponges to tackle this unique challenge.

Our DLD device performance mirrored that of work by Loutherback et al.[15] in two aspects: (1) that the theoretical change in critical diameter between the positive and negative row shifts does not seem to significantly impact our cell separation and (2) that high (mL/min) flow rates do not curtail cell separation. This finding is in slight contrast to simulations on triangular DLD arrays performed by Zhang *et al.* [18], which suggest the negative and positive arrays should have significantly different critical diameters (~6 μm difference). Another similar finding was that between flow rates of 10 μL/min and 5 mL/min, we did not observe much impact on cell separation efficacy (**Figure 3D**), suggesting that users can potentially complete the process within 30 seconds by manually pushing the syringe. This finding strongly supports the case for user-friendly DLD-based microfluidic separation as it demonstrates that high-precision of actuation is not needed, especially when selectivity between cell types is not a necessity. We believe this clearly allows for applications where the device can be syringe-driven by hand. Alternatively, the device can be redesigned to be driven by paper capillary pumps[16] or hydrostatic pressures via a reservoir near the inlet[26].

Although a higher cell concentration was achieved by incorporating a PDMS sponge for selective oil absorption, it was not a vital intervention as DLD device with PSAP beads alone led to extraction of similar amount of DNA from milk and PBS samples (**Figure 5F**). It should be noted, however, that special care was taken to avoid the milk fat at the top of the well when transferring liquid to an EM card sample area and it is possible to inadvertently pipette a large

quantity of undesired, cell-free milk fat in this step. Thus, PDMS sponges should be considered for convenience and improved reproducibility, particularly for milk samples with high fat contents. Together, the integration of viscosity-insensitive DLD design and the PDMS sponges significantly mitigates the large sample-to-sample variation in breastmilk.

Our results in **Figure 5E-F** clearly demonstrate that our target quantity of DNA (~1 μg) is collected and has potential to simplify DNA archiving from dilute physiological samples. Overall, our system is quite robust, simple, and has been shown to work properly with breastmilk from multiple women at relatively high flow rates. As our system leverages intentional lithographic patterning of DLD devices and "self-driven" cell enrichment of polymer beads and sponges rather than expensive control systems, we believe it can allow for effective and accessible cell enrichment in low resource, non-clinical settings.

DATA AVAILABILITY

The data underlying this article are either available in the article or will be shared on reasonable request to the corresponding authors.

ACKNOWLEDGMENTS

This work was partially supported by the NSF (CMMI-1846866 to Y.S.). Portions of this work were conducted in the Minnesota Nano Center, which is supported by the National Science Foundation through the National Nanotechnology Coordinated Infrastructure (NNCI) under Award Number ECCS-2025124. The fabrication was supported by an Explore Nano Grant from the Minnesota Nano Center to J. H.

CONFLICT OF INTEREST

The authors have declared that no conflict of interest exists.

FIGURE CAPTIONS

Figure 1: Schematic of the workflow for breastmilk cell analysis involving the microfluidic cell enrichment, placement of enriched solution on sample areas of EM card for DNA archiving, Water-based DNA elution from EM Card, DNA amplification using PCR, DNA sequencing and bisulfite sequencing Created with BioRender.com.

Figure 2: A.) DLD device design from Klayout (bottom) and brightfield image of device features. Scale bar, 500 μm. **B**.) Experimental setup with a DLD device mounted on an inverted microscope. Outlet tubings were attached to Eppendorf tubes for cell enriched and waste solution. **C**.) Mass Outflow rates during operation for cell outlet and waste outlet of the DLD device. **D**.) Cell concentration from the cell and waste outlet of the DLD device after operation.

Figure 3: A.) Phase contrast image of cells (outlined in red) flowing through the DLD device at 100 μL/min. Fluid is flowing from left to right. **B**.) Measurement of cell concentration of PBS from the cell outlet and waste outlet of the DLD device as well as the *status quo* and centrifuge experimental groups. **C**.) Cartoon schematic of syringe pump pushing milk through the DLD device and into Eppendorf tubes at four designated flow rates. **D**.) Cell concentration of PBS collected from the cell outlet of the DLD with respect to flow rate used. *, $P < 0.05$, **, $P < 0.01$, ***, $P < 0.001$, n.s., $P > 0.05$. Three experimental replicates were performed. Created with BioRender.com.

Figure 4: A.) Cartoon schematic of a PSAP bead selectively uptaking water and particles under 1 μm in diameter. **B**.) Dehydrated PSAP beads (right) and PSAP beads after 30 mins in DI water (left). **C**.) Image of DLD device integrated with dehydrated PSAP beads for hybrid cell enrichment (B-DLD). **D**.) Cartoon of PSAP cell enrichment of PBS in 24 well plate. **E**.) Comparison of fluid absorption efficacy in both PBS and breastmilk over 20 mins of immersion in 1 mL of either liquid. **F**.) Cell concentration of PBS from the *status quo*, DLD device combined with beads (B-DLD), and Centrifuge group. *, $P < 0.05$, **, $P < 0.01$, ***, $P < 0.001$, n.s., $P > 0.05$. Three experimental replicates were performed. Created with BioRender.com.

Figure 5: A.) 10× phase contrast image of breastmilk flowing through the DLD microfluidic device. Inserted box in red shows spherical milk fat globules entering the cell outlet of the device. **B**.) Fluorescence image of GFP-tagged MCF-7 cells entering the cell outlet of the DLD device. **C**.) PDMS sponges released from sugar templates **D**.) Cartoon depiction of milk fat globules rising above the continuous phase (water) of breastmilk, coalescing, and being absorbed into the pores of a hydrophobic PDMS sponge. Created with BioRender.com. **E**.) Bar graph of spectrophotometer readings of DNA concentration in PBS/breastmilk spiked with MDCK cells and processed using DLD, PSAP beads and/or PDMS sponges. *, $P < 0.05$, **, $P < 0.01$, ***, $P < 0.001$, n.s., $P > 0.05$. Three experimental replicates were performed. **F**.) DNA concentration readings from PCR amplification of *ALU* for blank breastmilk sample and breastmilk/PBS spiked with MCF-7 cells, and processed using DLD, PSAP beads and/or PDMS sponges.

FIGURES

Figure 1

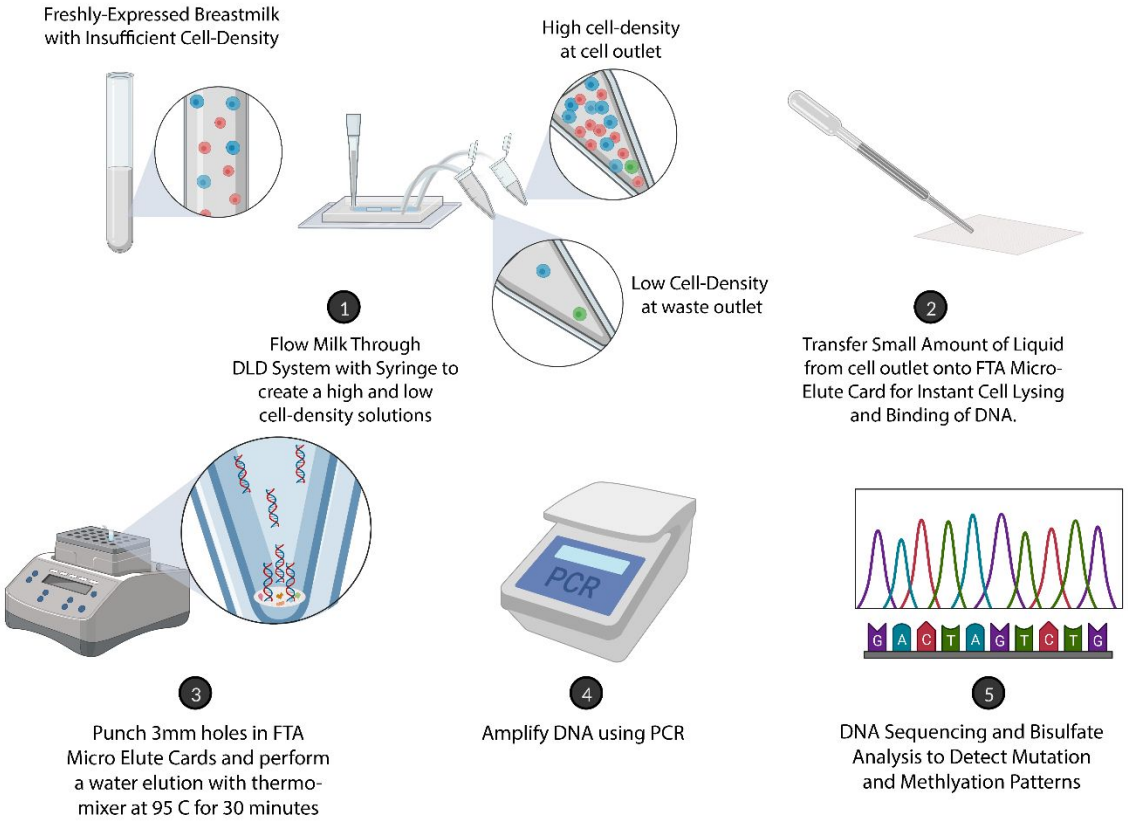

Figure 2

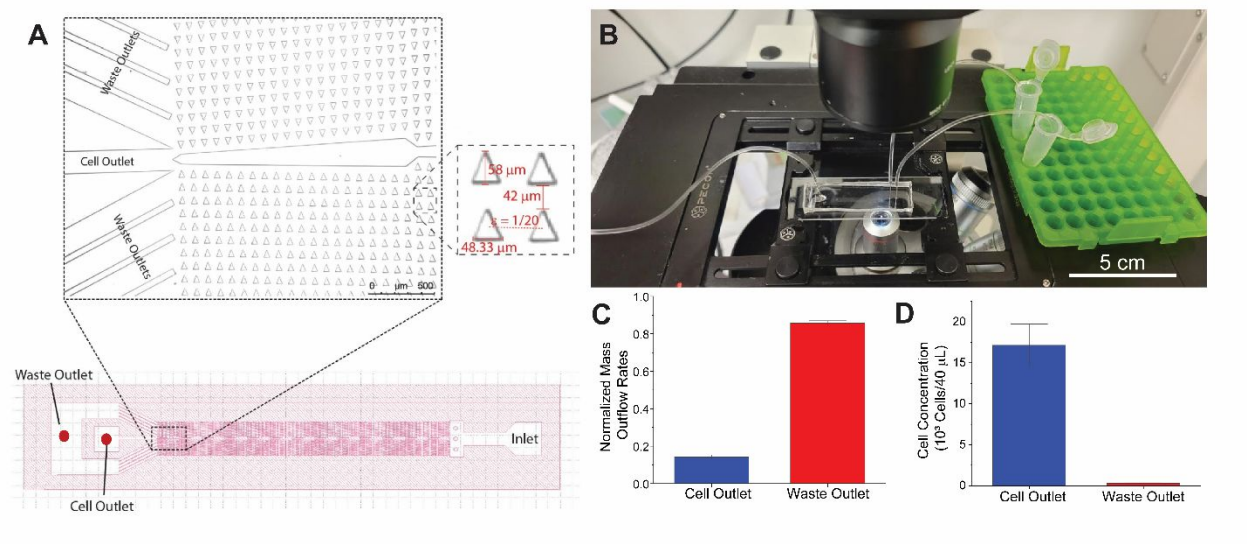
A
Waste Outlets
Cell Outlet
Waste Outlets
58 µm
42 µm
s = 1/20
48.33 µm
0 µm 600
Waste Outlet
Inlet
Cell Outlet
B
5 cm
C
Normalized Mass Outflow Rates
1.0
0.8
0.6
0.4
0.2
0.0
Cell Outlet
Waste Outlet
D
Cell Concentration (10³ Cells/40 µL)
20
15
10
5
0
Cell Outlet
Waste Outlet

Figure 3

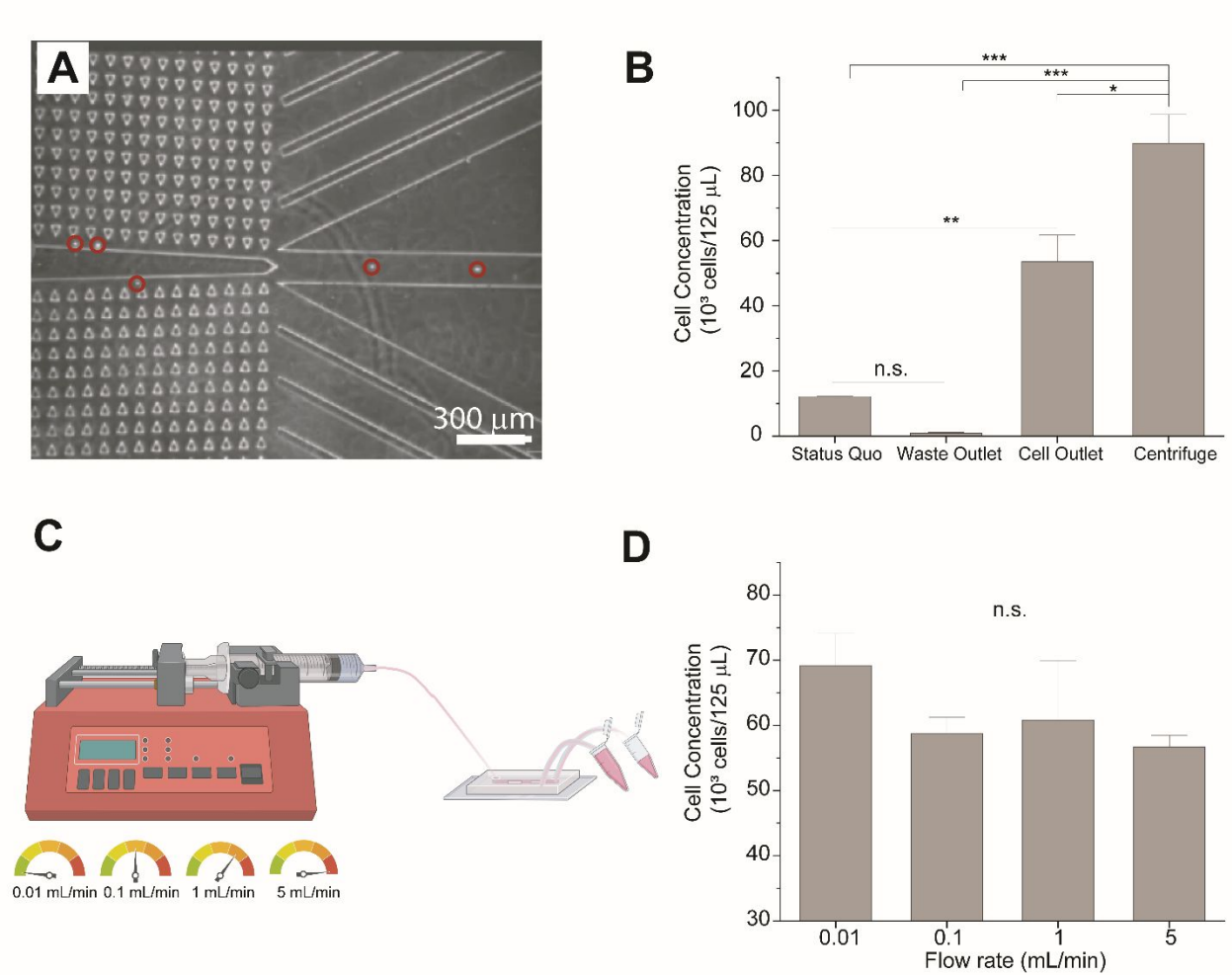
A
300 µm
B
***
***
*
**
n.s.
Cell Concentration (10³ cells/125 µL)
100
80
60
40
20
0
Status Quo
Waste Outlet
Cell Outlet
Centrifuge
C
0.01 mL/min
0.1 mL/min
1 mL/min
5 mL/min
D
n.s.
Cell Concentration (10³ cells/125 µL)
80
70
60
50
40
30
0.01
0.1
1
5
Flow rate (mL/min)

Figure 4

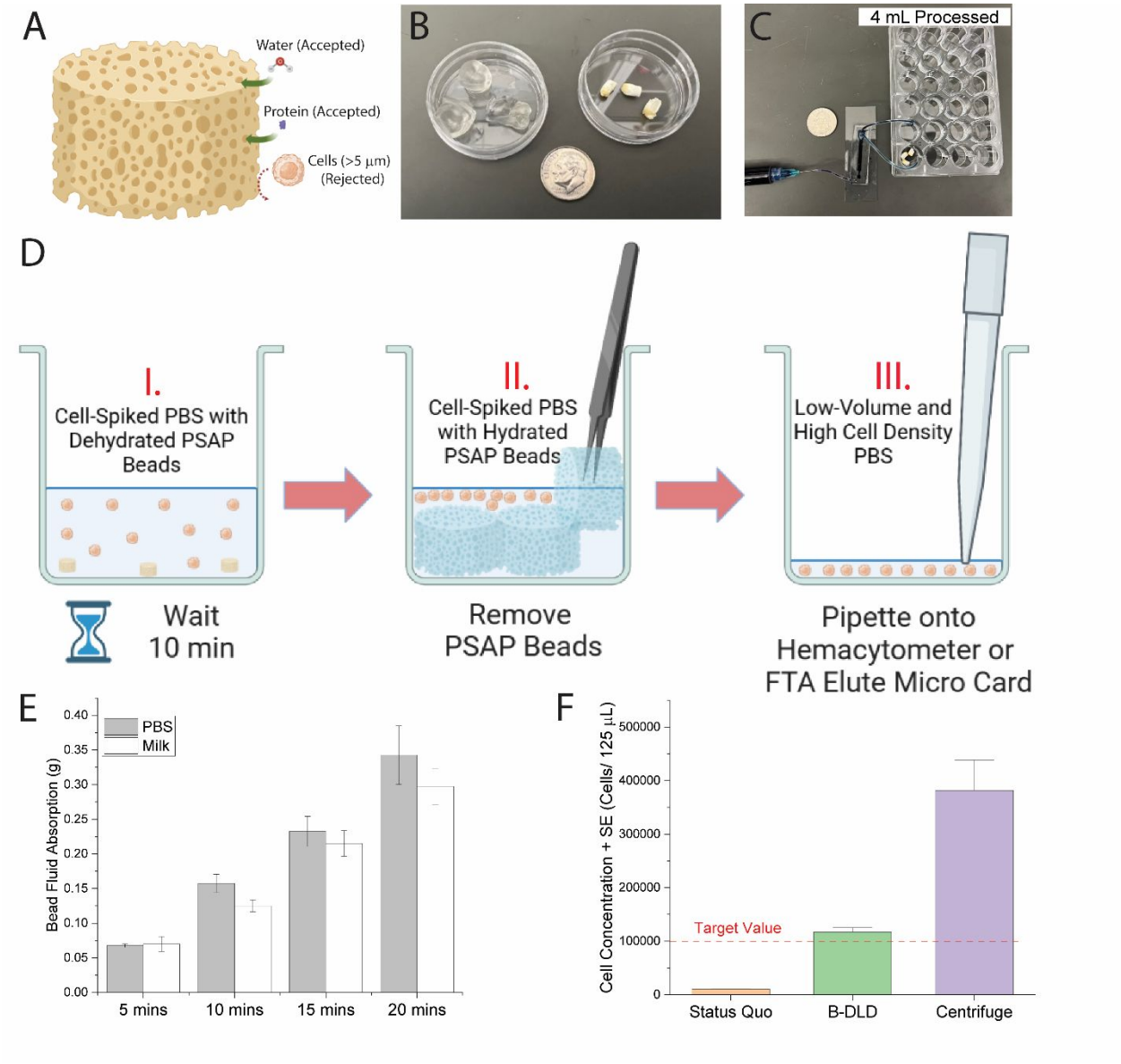
A
Water (Accepted)
Protein (Accepted)
Cells (>5 µm)
(Rejected)
B
C
4 mL Processed
D
I.
Cell-Spiked PBS with Dehydrated PSAP Beads
Wait 10 min
II.
Cell-Spiked PBS with Hydrated PSAP Beads
Remove PSAP Beads
III.
Low-Volume and High Cell Density PBS
Pipette onto Hemacytometer or FTA Elute Micro Card
E
PBS
Milk
Bead Fluid Absorption (g)
0.40
0.35
0.30
0.25
0.20
0.15
0.10
0.05
0.00
5 mins
10 mins
15 mins
20 mins
F
Cell Concentration + SE (Cells/ 125 µL)
500000
400000
300000
200000
100000
0
Target Value
Status Quo
B-DLD
Centrifuge

Figure 5

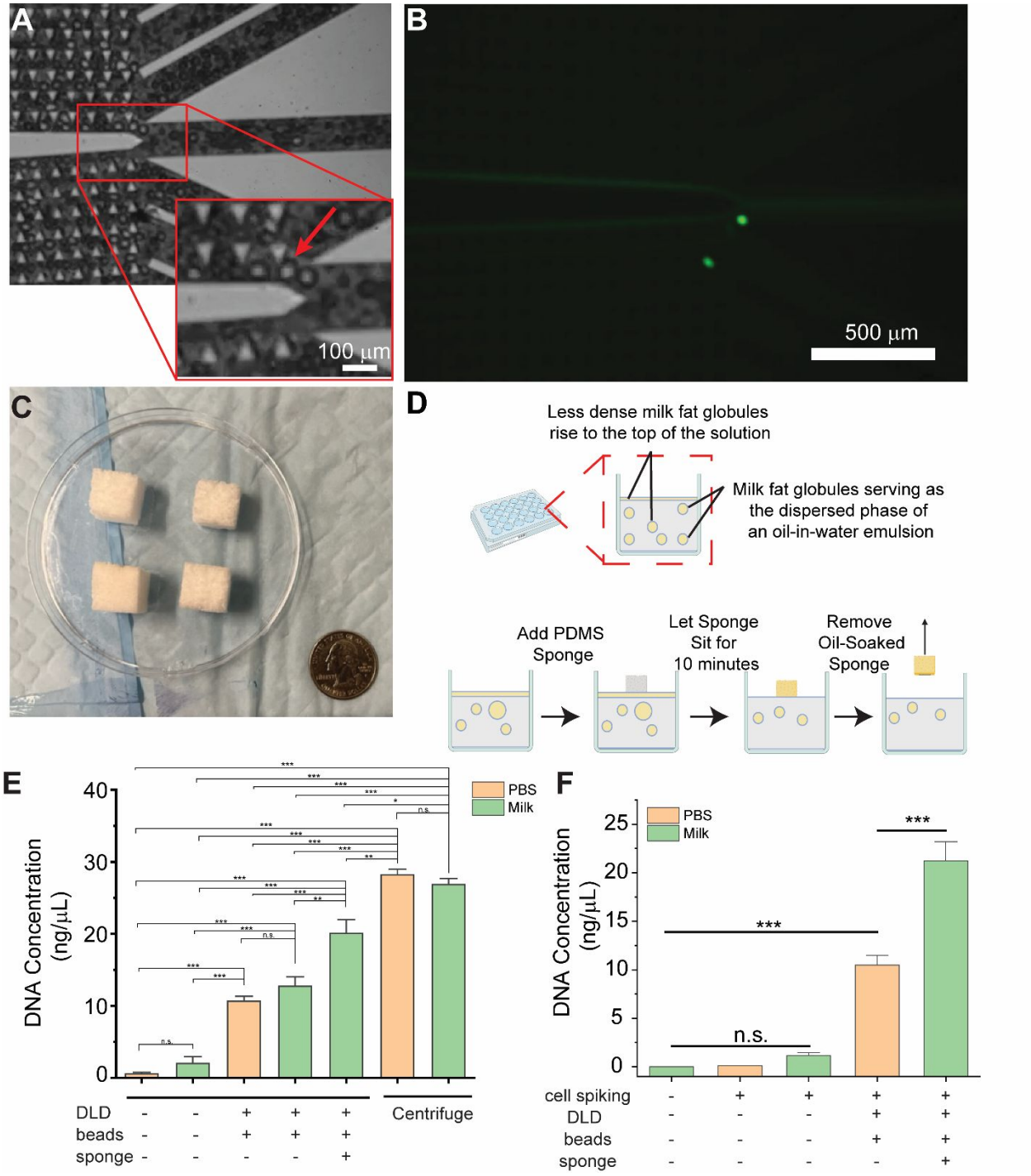
A
100 μm
B
500 μm
C
D
Less dense milk fat globules rise to the top of the solution
Milk fat globules serving as the dispersed phase of an oil-in-water emulsion
Add PDMS Sponge
Let Sponge Sit for 10 minutes
Remove Oil-Soaked Sponge
E
DNA Concentration (ng/μL)
PBS
Milk
DLD
beads
sponge
Centrifuge
F
DNA Concentration (ng/μL)
PBS
Milk
cell spiking
DLD
beads
sponge
n.s.
***

REFERENCES

1. H. B. Nichols, M. J. Schoemaker, J. Cai, J. Xu, L. B. Wright, M. N. Brook, M. E. Jones, H. O. Adami, L. Baglietto, K. A. Bertrand, W. J. Blot, M. C. Boutron-Ruault, M. Dorronsoro, L. Dossus, A. H. Eliassen, G. G. Giles, I. T. Gram, S. E. Hankinson, J. Hoffman-Bolton, R. Kaaks, T. J. Key, C. M. Kitahara, S. C. Larsson, M. Linet, M. A. Merritt, R. L. Milne, V. Pala, J. R. Palmer, P. H. Peeters, E. Riboli, M. Sund, R. M. Tamimi, A. Tjønneland, A. Trichopoulou, G. Ursin, L. Vatten, K. Visvanathan, E. Weiderpass, A. Wolk, W. Zheng, C. R. Weinberg, A. J. Swerdlow and D. P. Sandler, *Ann Intern Med*, 2019, **170**, 22-30.
2. E. B. Callihan, D. Gao, S. Jindal, T. R. Lyons, E. Manthey, S. Edgerton, A. Urquhart, P. Schedin and V. F. Borges, *Breast Cancer Res Treat*, 2013, **138**, 549-559.
3. E. T. Goddard, R. C. Hill, T. Nemkov, A. D'Alessandro, K. C. Hansen, O. Maller, S. Mongoue-Tchokote, M. Mori, A. H. Partridge, V. F. Borges and P. Schedin, *Cancer Discovery*, 2017, **7**, 177-187.
4. A. L. Johansson, T. M. Andersson, C. C. Hsieh, S. Cnattingius and M. Lambe, *Cancer epidemiology, biomarkers & prevention : a publication of the American Association for Cancer Research, cosponsored by the American Society of Preventive Oncology*, 2011, **20**, 1865-1872.
5. B. P. de Almeida, J. D. Apolónio, A. Binnie and P. Castelo-Branco, *Bmc Cancer*, 2019, **19**, 219.
6. L. A. Salas, S. N. Lundgren, E. P. Browne, E. C. Punska, D. L. Anderton, M. R. Karagas, K. F. Arcaro and B. C. Christensen, *Human Molecular Genetics*, 2020, **29**, 662-673.
7. K. P. M. Suijkerbuijk, P. J. van Diest and E. van der Wall, *Annals of Oncology*, 2011, **22**, 24-29.
8. I. Schultz-Pernice, L. K. Engelbrecht, S. Petricca, C. H. Scheel and A. J. Twigger, *J Mammary Gland Biol Neoplasia*, 2020, **25**, 397-408.
9. J. P. Gleeson, N. Chaudhary, K. C. Fein, R. Doerfler, P. Hredzak-Showalter and K. A. Whitehead, *Sci Adv*, 2022, **8**, eabm6865.
10. T. Keller, L. Wengenroth, D. Smorra, K. Probst, L. Kurian, A. Kribs and B. Brachvogel, *Cytometry B Clin Cytom*, 2019, **96**, 480-489.
11. D. C. Koboldt, R. S. Fulton, M. D. McLellan, H. Schmidt, J. Kalicki-Veizer, J. F. McMichael, L. L. Fulton, D. J. Dooling, L. Ding, E. R. Mardis, R. K. Wilson, A. Ally, M. Balasundaram, Y. S. N. Butterfield, R. Carlsen, C. Carter, A. Chu, E. Chuah, H.-J. E. Chun, R. J. N. Coope, N. Dhalla, R. Guin, C. Hirst, M. Hirst, R. A. Holt, D. Lee, H. I. Li, M. Mayo, R. A. Moore, A. J. Mungall, E. Pleasance, A. Gordon Robertson, J. E. Schein, A. Shafiei, P. Sipahimalani, J. R. Slobodan, D. Stoll, A. Tam, N. Thiessen, R. J. Varhol, N. Wye, T. Zeng, Y. Zhao, I. Birol, S. J. M. Jones, M. A. Marra, A. D. Cherniack, G. Saksena, R. C. Onofrio, N. H. Pho, S. L. Carter, S. E. Schumacher, B. Tabak, B. Hernandez, J. Gentry, H. Nguyen, A. Crenshaw, K. Ardlie, R. Beroukhim, W. Winckler, G. Getz, S. B. Gabriel, M. Meyerson, L. Chin, P. J. Park, R. Kucherlapati, K. A. Hoadley, J. Todd Auman, C. Fan, Y. J. Turman, Y. Shi, L. Li, M. D. Topal, X. He, H.-H. Chao, A. Prat, G. O. Silva, M. D. Iglesia, W. Zhao, J. Usary, J. S. Berg, M. Adams, J. Booker, J. Wu, A. Gulabani, T. Bodenheimer, A. P. Hoyle, J. V. Simons, M. G. Soloway, L. E. Mose, S. R. Jefferys, S. Balu, J. S. Parker, D. Neil Hayes, C. M. Perou, S. Malik, S. Mahurkar, H. Shen, D. J. Weisenberger, T. Triche Jr, P. H. Lai, M. S. Bootwalla, D. T. Maglinte, B. P. Berman, D. J. Van Den Berg, S. B. Baylin, P. W. Laird, C. J. Creighton, L. A. Donehower, G. Getz, M. Noble, D. Voet, G. Saksena, N. Gehlenborg, D. DiCara, J. Zhang, H. Zhang, C.-J. Wu, S. Yingchun Liu, M. S. Lawrence, L. Zou, A. Sivachenko, P. Lin, P. Stojanov, R. Jing, J. Cho, R. Sinha, R. W. Park, M.-D. Nazaire, J. Robinson, H. Thorvaldsdottir, J. Mesirov, P. J. Park, L. Chin, S. Reynolds, R. B. Kreisberg, B. Bernard, R. Bressler, T. Erkkila, J. Lin, V. Thorsson, W. Zhang, I. Shmulevich, G. Ciriello, N. Weinhold, N. Schultz, J. Gao, E. Cerami, B. Gross, A. Jacobsen, R. Sinha, B. Arman Aksoy, Y. Antipin, B. Reva, R. Shen, B. S. Taylor, M. Ladanyi, C. Sander, P. Anur, P. T. Spellman, Y. Lu, W. Liu, R. R. G. Verhaak, G. B. Mills, R. Akbani, N. Zhang, B. M. Broom, T. D. Casasent, C. Wakefield, A. K. Unruh, K. Baggerly, K. Coombes, J. N. Weinstein, D. Haussler, C. C. Benz, J. M. Stuart, S. C. Benz, J. Zhu, C. C. Szeto, G. K. Scott, C. Yau, E. O. Paull, D. Carlin, C. Wong, A. Sokolov, J. Thusberg, S. Mooney, S. Ng, T. C. Goldstein, K. Ellrott, M. Grifford, C. Wilks, S. Ma, B. Craft, C. Yan, Y. Hu, D. Meerzaman, J. M. Gastier-Foster, J. Bowen, N. C. Ramirez, A. D. Black, R. E. Pyatt, P. White, E. J. Zmuda, J. Frick, T. M. Lichtenberg, R. Brookens, M. M. George, M. A. Gerken, H. A. Harper, K. M. Leraas, L. J. Wise, T. R. Tabler, C. McAllister, T. Barr, M. Hart-Kothari, K. Tarvin, C. Saller, G. Sandusky, C. Mitchell, M. V. Iacocca, J. Brown, B. Rabeno, C. Czerwinski, N. Petrelli, O. Dolzhansky, M. Abramov, O. Voronina, O. Potapova, J. R. Marks, W. M. Suchorska, D. Murawa, W. Kycler, M. Ibbs, K. Korski, A. Spychała, P. Murawa, J. J. Brzeziński, H. Perz, R. Łaźniak, M. Teresiak, H. Tatka, E. Leporowska, M. Bogusz-Czerniewicz, J. Malicki, A. Mackiewicz, M. Wiznerowicz, X. Van Le,

B. Kohl, N. Viet Tien, R. Thorp, N. Van Bang, H. Sussman, B. Duc Phu, R. Hajek, N. Phi Hung, T. Viet The Phuong, H. Quyet Thang, K. Zaki Khan, R. Penny, D. Mallery, E. Curley, C. Shelton, P. Yena, J. N. Ingle, F. J. Couch, W. L. Lingle, T. A. King, A. Maria Gonzalez-Angulo, G. B. Mills, M. D. Dyer, S. Liu, X. Meng, M. Patangan, N. The Cancer Genome Atlas, L. Genome sequencing centres: Washington University in St, B. C. C. A. Genome characterization centres, I. Broad, Brigham, H. Women's, S. Harvard Medical, C. H. University of North Carolina, H. University of Southern California/Johns, M. Genome data analysis: Baylor College of, B. Institute for Systems, C. Memorial Sloan-Kettering Cancer, H. Oregon, U. Science, M. D. A. C. C. The University of Texas, S. C. B. I. University of California, Nci, R. Biospecimen core resource: Nationwide Children's Hospital Biospecimen Core, A.-I. Tissue source sites, Christiana, Cureline, C. Duke University Medical, C. The Greater Poland Cancer, Ilsbio, C. International Genomics, C. Mayo, Mskcc and M. D. A. C. Center, *Nature*, 2012, **490**, 61-70.

12. B. C. Davis Lynn, C. Bodelon, R. M. Pfeiffer, H. P. Yang, H. H. Yang, M. Lee, P. W. Laird, M. Campan, D. J. Weisenberger, J. Murphy, J. N. Sampson, E. P. Browne, D. L. Anderton, M. E. Sherman, K. F. Arcaro and G. L. Gierach, *Cancer Prev Res (Phila)*, 2019, **12**, 781-790.
13. P. Li, Z. Mao, Z. Peng, L. Zhou, Y. Chen, P.-H. Huang, C. I. Truica, J. J. Drabick, W. S. El-Deiry, M. Dao, S. Suresh and T. J. Huang, *Proceedings of the National Academy of Sciences*, 2015, **112**, 4970-4975.
14. D. Di Carlo, D. Irimia, R. G. Tompkins and M. Toner, *Proc Natl Acad Sci U S A*, 2007, **104**, 18892-18897.
15. K. Loutherback, J. D'Silva, L. Liu, A. Wu, R. H. Austin and J. C. Sturm, *AIP Advances*, 2012, **2**, 042107.
16. T. S. H. Tran, B. D. Ho, J. P. Beech and J. O. Tegenfeldt, *Lab Chip*, 2017, **17**, 3592-3600.
17. J. A. Davis, *Microfluidic separation of blood components through deterministic lateral displacement*, Princeton University, 2008.
18. Z. Zhang, E. Henry, G. Gompper and D. A. Fedosov, *The Journal of Chemical Physics*, 2015, **143**, 243145.
19. K. Loutherback, K. S. Chou, J. Newman, J. Puchalla, R. H. Austin and J. C. Sturm, *Microfluidics and Nanofluidics*, 2010, **9**, 1143-1149.
20. W. Chen, T. Wang, Z. Dou and X. Xie, *ACS Materials Letters*, 2020, **2**, 1545-1554.
21. C. Lopez, C. Cauty and F. Guyomarc'h, *European Journal of Lipid Science and Technology*, 2019, **121**, 1800201.
22. A. T. S. A. I. I. V. Murray., *Histology, White Blood Cell.*, StatPearls Publishing, Treasure Island (FL), 2022.
23. X. Wu, X. Huang, Y. Zhu, J. Li and M. R. Hoffmann, *Separation and purification technology*, 2020, **239**, 116540.
24. H. C. Yang, Y. M. Ham, J. A. Kim and W. J. Rhee, *Journal of Extracellular Vesicles*, 2021, **10**, e12074.
25. N. Gawande and A. A. Mungray, *Separation and purification technology*, 2015, **150**, 86-94.
26. M. Komeya, K. Hayashi, H. Nakamura, H. Yamanaka, H. Sanjo, K. Kojima, T. Sato, M. Yao, H. Kimura, T. Fujii and T. Ogawa, *Sci Rep*, 2017, **7**, 15459.